



**Michigan
Technological
University**

Michigan Technological University
Digital Commons @ Michigan Tech

Michigan Tech Publications

8-2022

Challenges of modeling rainfall triggered landslides in a data-sparse region: A case study from the Western Ghats, India

C. L. Vishnu

Michigan Technological University

T. Oommen

Michigan Technological University, toommen@mtu.edu

Snehamoy Chatterjee

Michigan Technological University, schatte1@mtu.edu

K. S. Sajinkumar

Michigan Technological University, skochapp@mtu.edu

Follow this and additional works at: <https://digitalcommons.mtu.edu/michigantech-p>



Part of the [Geological Engineering Commons](#), and the [Mining Engineering Commons](#)

Recommended Citation

Vishnu, C., Oommen, T., Chatterjee, S., & Sajinkumar, K. (2022). Challenges of modeling rainfall triggered landslides in a data-sparse region: A case study from the Western Ghats, India. *Geosystems and Geoenvironment*, 1(3). <http://doi.org/10.1016/j.geogeo.2022.100060>

Retrieved from: <https://digitalcommons.mtu.edu/michigantech-p/16096>

Follow this and additional works at: <https://digitalcommons.mtu.edu/michigantech-p>



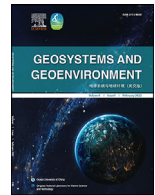
Part of the [Geological Engineering Commons](#), and the [Mining Engineering Commons](#)



ELSEVIER

Contents lists available at ScienceDirect

Geosystems and Geoenvironment

journal homepage: www.elsevier.com/locate/geogeo

Challenges of modeling rainfall triggered landslides in a data-sparse region: A case study from the Western Ghats, India

C.L. Vishnu^a, T. Oommen^a, S. Chatterjee^a, K.S. Sajinkumar^{a,b,*}^a Department of Geological and Mining Engineering and Sciences, Michigan Technological University, Houghton, MI, USA^b Department of Geology, University of Kerala, Thiruvananthapuram, Kerala 695581, India

ARTICLE INFO

Article history:

Received 12 January 2022

Revised 17 February 2022

Accepted 25 March 2022

Keywords:

Landslides

GPM

IMERG

Conditional merging

Remote sensing

Satellite precipitation

ABSTRACT

Accurate rainfall estimates are required to forecast the spatio-temporal distribution of rain-triggered landslides. In this study, a comparison between rain gauge and satellite rainfall data for assessing landslide distribution in a data-sparse region, the mountainous district of Idukki, along the Western Ghats of south-western India, is carried out. Global Precipitation Mission Integrated Multi-satellite Retrievals for GPM-Late (GPM IMERG-L) rainfall products were compared with rain gauge measurements, and it was found that the satellite rainfall observations were underpredicting the actual rainfall. A conditional merging algorithm was applied to develop a product that combines the accuracy of rain gauges and the spatial variability of satellite precipitation data. Correlation Coefficient (CC) and Root Mean Squared Error (RMSE) were used to check the performance of the conditional merging process. An example from a station with the least favorable statistics shows the CC increasing from 0.589 to 0.974 and the RMSE decreasing from 65.22 to 20.01. A case scenario was considered that evaluated the performance of a landslide prediction model by relying solely on a sparse rain gauge network. Rainfall thresholds computed from both the conditionally merged GPM IMERG-L and the rain gauge data were compared and the differences indicated that relying solely on a discrete, sparse rain gauge network would create false predictions. A total of 18.7% of landslide predictions only were identified as true positives, while 60.7% was the overall false-negative rate, and the remaining were false-positives. This pointed towards the need of having a continuous data that is both accurate in measurement and efficient in capturing spatial variability of rainfall.

© 2022 The Author(s). Published by Elsevier Ltd on behalf of Ocean University of China.

This is an open access article under the CC BY license (<http://creativecommons.org/licenses/by/4.0/>)

1. Introduction

Landslides occur due to decreased slope stability and are triggered by seismic activity, snow melting, or heavy rainfall (Guzzetti et al., 2002). Rain can increase the piezometric surface, causing increased pore-pressure and decreased soil shear resistance, leading to slope failures (Arnone et al., 2011). 75% of rain-induced landslides in the world occur in developing Asian countries, including China and the Indian subcontinent, claiming, on average, 500 lives and causing property loss of about 3 billion U.S. dollars every year (Froude and Petley, 2018).

The Western Ghats in southwest India is one of the most landslide-prone areas (Abraham and Shaji, 2013; Sajinkumar et al., 2020; Sajinkumar and Oommen, 2021) and is characterized by rugged hills and steep slopes (Sajinkumar et al., 2011). The West-

ern Ghats receive an annual average rainfall of above 3000 mm, a major triggering factor for landslides (Thampi, 1997). This can be exemplified through the recent incidence during August 2018 when a major part of the Western Ghats received heavy rainfall that resulted in floods and landslides that took hundreds of lives (Vishnu et al., 2019, 2020; Jennifer and Saravanan, 2021; Sajinkumar et al., 2022). Idukki, a district nestled in the Western Ghats, alone recorded 2223 landslides in August 2018 (Hao et al., 2020). The years 2019 and 2020 also witnessed frequent landslides. A major landslide in Malappuram, Kerala, in 2019 claimed 69 lives (Wadhawan et al., 2020), while a landslide in Idukki in 2020 claimed more than 50 lives (Sajinkumar and Oommen, 2020). This calls for developing a landslide early warning model that utilizes rainfall measurements and slope stability analysis to forecast landslide occurrences.

However, Idukki has a sparse rain gauge network with just five rain gauges over an area of 4366 sq. km. Such a sparse network creates many challenges in accurately creating a landslide model as the landslides in Idukki are predominantly rain-triggered.

* Corresponding author at: Department of Geological and Mining Engineering and Sciences, Michigan Technological University, Houghton, MI, USA.

E-mail address: sajinks@keralauniversity.ac.in (K.S. Sajinkumar).

Limitations in accurate landslide prediction models adversely affect the early warning systems, resulting in generating false warnings. False negatives would give rise to catastrophic outcomes claiming lives and property whereas false positives would reduce the population's faith in scientific warnings and could lead them to gradually begin ignoring warnings, because of warning fatigue (Sorensen and Sorensen, 2007; Dash and Gladwin, 2007; Mackie, 2014) and cause disastrous consequences. Thus, it is equally important for the scientific community and policymakers to improve rainfall measurements.

Developing a landslide early warning system includes two steps: modeling slope stability and modeling rainfall thresholds that trigger the landslides (Stanley and Kirschbaum, 2017; Naidu et al., 2018). Most of the current landslide models combine slope stability model and hydrologic model, including HYSWASOR (Dirksen et al., 1993), TOPMODEL (Lamb et al., 1998), SHALSTAB (Dietrich and Montgomery, 1998), Antecedent Soil Water Status (ASWSM) (Crozier, 1999), SINMAP (Pack et al., 2001) and tRIBS VEGGIE (Lepore et al., 2013) models. Rainfall thresholds are also established using statistical approaches such as Larsen and Simon (1993), Terlien (1998), Glade et al. (2000), and Kim et al. (2010). Iverson (2000) established the significance of rainfall infiltration in triggering shallow landslides and pitched for accurate rainfall estimates and landslide catalogs for rain-triggered landslide modeling. Hong et al. (2007) pointed out the significance of a rainfall product with a sufficient temporal resolution, a comprehensive land surface database, a hydrological modeling component, and a landslide database to develop a rain-triggered landslide model.

The predominant source of rainfall measure is rain gauges. However, most of the world's mountainous parts, especially in developing countries, have sparse rain gauge networks and fail to capture rainfall's spatial variability (Sinclair and Pegram, 2005). Sidle and Ochia (2006) observed the need to develop better rain estimation networks in developing countries to improve landslide modeling and early warning systems. In India, rain gauges are predominantly operated by India Meteorological Department (IMD). Mishra (2013) performed an accuracy analysis on the IMD operated Automated Weather Stations (AWS) and inferred that with increase in gauge spacing larger variations in rainfall were identified. The study identified 15 km as an upper limit for observing significant spatial variations in rainfall. Mishra (2013) concluded gauge spacing as an essential parameter for the accurate representation of rainfall using the rain gauges. The study also identified the importance of using gauge adjusted satellite data for filling the gaps occurring due to poor rain gauge density. Prakash et al. (2019) identified rain gauge density and spatial variation in rainfall as two factors that contributed to the uncertainty in rainfall observations in India. The study identified NE India as having the least rain gauge density while South India as having the largest spatial variation in rainfall. It should be noted that even though South India in general have denser rain gauge networks, the mountainous regions of Idukki is an exception. Prakash et al. (2015) compared seven gridded rainfall datasets with the IMD gridded rainfall as reference. The study observed largest uncertainties in orographic regions including the Western Ghats. The IMD gridded dataset is a spatially interpolated gridded product derived from about 3500 quality-controlled rain gauge observations on an average on a daily timescale at a spatial resolution of 50 km over the Indian region (Rajeevan and Bhat, 2009). Even though various studies (Joshi et al., 2013; Gairola et al., 2015; Parida et al., 2017) used the gridded rainfall product derived from IMD stations as reference for comparing the quality of various rainfall products over India, the different rain gauge densities in different parts of the country owes to certain uncertainty in the gridded product.

Studies also turned towards radar or satellite-based precipitation measures that efficiently capture the spatial variability of rainfall in relatively high spatial and temporal resolutions (Guenzi et al., 2017). While radar measurements are subjected to a series of errors like beam blockage and wave attenuation, especially in mountainous terrain, satellite measurements provide calibrated global coverage (Kirschbaum and Stanley, 2018; Tang et al., 2020). Hong and Adler (2008) developed the first satellite-based model for rain-triggered landslides globally using the Tropical Rainfall Measuring Mission (TRMM) data product (Garstang and Kummerow, 2000; Liu et al., 2012). TRMM, a joint venture of NASA and JAXA, provided satellite rainfall measures from 1997 to 2015. TRMM is now succeeded by a multi-satellite precipitation monitoring system, the Global Precipitation Mission (GPM) (Hou et al., 2014; Liu et al., 2017). The study by Hong and Adler (2008) was followed by many that compared and analyzed the performance of satellite data with conventional rain gauge networks (Marra et al., 2014; Rossi et al., 2012). However, such studies had a general inference that pointed towards the overestimation of light rainfall and underestimation of heavy rainfall by satellite products (Nikolopoulos et al., 2017; Robbins, 2016). Brunetti et al. (2018) compared various rainfall products for their ability in forecasting landslides over Italy and found that the Climate Prediction center (CPC) Morphing Technique (CMORPH) and the SM2RAIN Advanced SCATterometer (ASCAT) products as the best performing. However, the observations were still underpredicting rainfall and the thresholds had to be adjusted accordingly to forecast landslides. A later study by Brunetti et al. (2021) analyzed various satellite products for predicting landslides in India and inferred that a merged GPM and SM2RAIN ASCAT product provided the better results. Pradhan and Indu (2021) identified that GPM IMERG performed better in orographic regions like the Western Ghats during the monsoons while SM2RAIN performed better during the pre-monsoon season.

Though the satellite precipitation measures provide high global coverage and spatial variability, they lack accurate rainfall estimates (Vignal and Krajewski, 2001). This occurs due to biases that predominantly result from the satellite precipitation being a result of atmospheric observations modeled using certain algorithm to eventually produce precipitation measurements (Boushaki et al., 2009). The lack of accuracy in rainfall estimates from satellite data poses a significant challenge for precipitation data retrieval and often calls for the bias adjustment of satellite precipitation. Zambrano-Bigiarini et al. (2017) noted that the satellite precipitation should be validated on a case-by-case basis. Adjusting satellite rainfall products generally follows two paths: using gauge measurements and using different satellite precipitation measurements where gauge measurements are not available. Satellite precipitation products often comes with internal bias correction procedures as is done by IMERG that uses monthly gauge data to adjust the precipitation measures (Tang et al., 2020). However, the monthly timescale is often too coarse and precipitation bias correction on daily or hourly timescale is required. Tobin and Bennett (2010) noticed the inadequacy of TRMM and the CMORPH algorithm in effectively capturing precipitations and developed a process that used ground precipitation data and probability filtering techniques to condition satellite data. Boushaki et al. (2009) used the gauge measurements from the Climate Prediction Center (CPC) to adjust satellite precipitation. The adjustment was based on calculating an error field that gave a weighted difference between the satellite and CPC rainfall with the weightage factor being the inverse distance from the CPC grids. Zhao et al. (2018) compared six satellite precipitation products over mainland China and observed that gauge adjusted GSMAP and GPM IMERG performed better. Sungmin and Kirstetter (2018) identified that the gauge adjusted IMERG-F version performed the best among the IMERG ver-

sions. Nikolopoulos et al. (2017) noted the need to merge rain gauge and satellite data products to combine the accuracy of rain gauges and spatial variability of satellite data to predict better rainfall-triggered landslides. In recent years, machine learning has been used to combine heterogeneous data sources (Guarascio et al., 2020). Woldemeskel et al. (2013) used a linearized weightage procedure to combine modified inverse distance weighted (IDW) rain gauge interpolated product with satellite rainfall product. However, Sinclair and Pegram (2005) noted that due to the fractal variability of rainfall in space, simple interpolation of rain gauges is unable to capture the spatial field of rainfall accurately. Conditional Merging (Pegram and Clothier, 2001; Sinclair and Pegram, 2005) is a widely used successful method (Berndt et al., 2014) to merge radar observations with rain gauge measurements. This method uses ordinary kriging to interpolate the rain gauge values and later combines it with the radar/satellite data's spatial structure (Sinclair and Pegram, 2005).

This study analyzed the utility of rain gauge and satellite data in Idukki for modeling rain-triggered landslides. The region receives an abundance of rainfall and is subjected to shallow landslides, especially during the monsoon seasons but has sparse rain gauge density with only five rain gauge stations for over 4366 sq. km. The study considers a landslide database created by Hao et al. (2020), corresponding to the August 2018 anomalous rainfall. This study compares rain gauge and satellite rainfall measures to the landslide occurrence pattern to assess optimal rainfall data for landslide modeling and early warning. This objective is achieved using the following steps on a case study in Idukki with sparse rain gauge data:

- (a) Compare rain gauge and satellite data for the Idukki region.
- (b) Perform conditional merging on satellite data and analyze how this changes satellite rainfall products' performance with respect to rain gauge measurements.
- (c) Compare between rain gauge observations and conditionally merged satellite data for predicting landslide distribution.

2. Study area

In the Western Ghats (Fig. 1a), the Idukki district is one of the densely populated districts with a population of 1.11 million and 254 inhabitants per sq. km. Idukki exhibits two of the three physiographic divisions viz., midlands (7.5–75 m amsl), and highlands (>75 m amsl). Owing to high population density, people are forced to move to the highlands, leading to an increase in anthropogenic stress on the slopes. The most seen human influence on vulnerable slopes is cut slope and land clearance for constructional purposes. Jones et al. (2021) observes anthropogenic factors such as land use, road density and quarry density as major factors for increased landslide susceptibility in Idukki. Kuriakose et al. (2009) indicates that the deforestation rates prevailing from the 19th century as a predominant force in increasing the landslide susceptibility of the region. Idukki experiences an annual average of 4100 mm of rainfall, with most of the rain occurring during the south-west monsoon from June to September. In 2018, from the 1st of June to the 29th of August, anomalously high rainfalls, with a departure of 36% above the average rainfall measure, were reported (Vishnu et al., 2019). This anomalous rainfall caused heavy floods and landslides, claiming massive loss of life and property. This point towards developing a landslide early warning system for mitigating such disaster. However, the sparse rain gauge network poses a challenge in acquiring data with enough spatial variability to model landslides (Fig. 1b). Table 1 shows the location of the rain gauges with latitude, longitude, and elevation values.

Table 1
Location and elevation details of rain gauges in Idukki, Kerala.

Station Name	Latitude (°N)	Longitude (°E)	Elevation (m)
Peermade	9.5667	76.9833	1000
Thodupuzha	9.8983	76.7131	37
Munnar	10.0000	77.1500	1175
Idukki	9.8333	76.9167	926
Myladumpara	9.6851	77.1851	1095

3. Data and methods

Rain gauge measurements were obtained from IMD (www.imd.gov.in). Though many studies relied on the IMD gridded data, this study opted to use the actual rain gauge data corresponding to the ground reality as the gridded product is an interpolation of this actual data. Five such rain gauges in the Idukki district were considered for this study. Daily data for August 2018 was taken and missing data were imputed by arithmetic average of daily rainfall over the stations. GPM Integrated Multi-satellitE Retrievals for GPM-Late (IMERG-L) daily data was downloaded from the official site for GPM downloads using an earth data account (www.gpm.nasa.gov). Landslide data for 2018 was taken from Hao et al. (2020). SRTM 30 m DEM was used for elevation calculations.

GPM is a constellation of satellites that use active radar, passive microwave, and infrared imaging to acquire global precipitation measures. These satellites provide precipitation measures for every 30 min for >90% of the earth. The core observatory is a combined enterprise by NASA and JAXA. It consists of a Dual-frequency Precipitation Radar (DPR) operating on K and Ka bands and a GPM Microwave Imager (GMI). The GPM provides four levels of data products: Level 1 consists of inter-calibrated and geolocated brightness temperatures from DPR, GMI, and other partner radiometers; Level 2 consists of intercalibrated precipitation rates; Level 3 consists of gridded time-space precipitation rates and latent heats, combining data from core observatory and other partners using a multi-satellite merging algorithm (IMERG); Level 4 is a research product created from merging remote sensing data and model inputs (Hou et al., 2014). The IMERG products, in turn, give three levels of products: the near real-time 4 h latency 'Early' (IMERG-E) and 14 h latency 'Late' (IMERG-L) products and the post-real-time research ready 'Final' (IMERG-F) product, at a spatio-temporal resolution of 0.1°×0.5 h (Sun et al., 2018). The products are available at hourly, daily, and monthly precipitation rates (More details of GPM data are available in https://disc.gsfc.nasa.gov/datasets/GPM_3IMERGDL_06/summary?keywords=imerg). The research-ready product is available at a latency of about 40 days and cannot be used for near real-time modeling. Early warning systems need near-real-time input. Therefore, in this study, we have utilized the IMERG-L daily product for August 2018 as this period corresponds to the events in the landslide database.

To establish the difference between rain gauge and satellite data products, the satellite pixel value corresponding to the rain gauge locations were compared with the actual rain gauge measures. Previous literature on the study area (Sajinkumar et al., 2020) considered antecedent rainfall over 2, 3, and 5 days to arrive at rainfall thresholds to model landslides and found that the 5-day antecedent rainfall performed better. Thus, in this study, we opted to choose a 5-day antecedent period as the threshold for the landslides to compare the rain gauge and satellite rainfall measurements. Therefore, a comparison between range gauge and GPM IMERG-L precipitation measurement was carried out for a daily timestep and cumulative 5-day antecedent periods. 5-day antecedent values were computed for all dates from 6th August to 31st August. Pearson's correlation coefficients (CC) and Root Mean Squared Errors (RMSE) were calculated between the rain gauge and

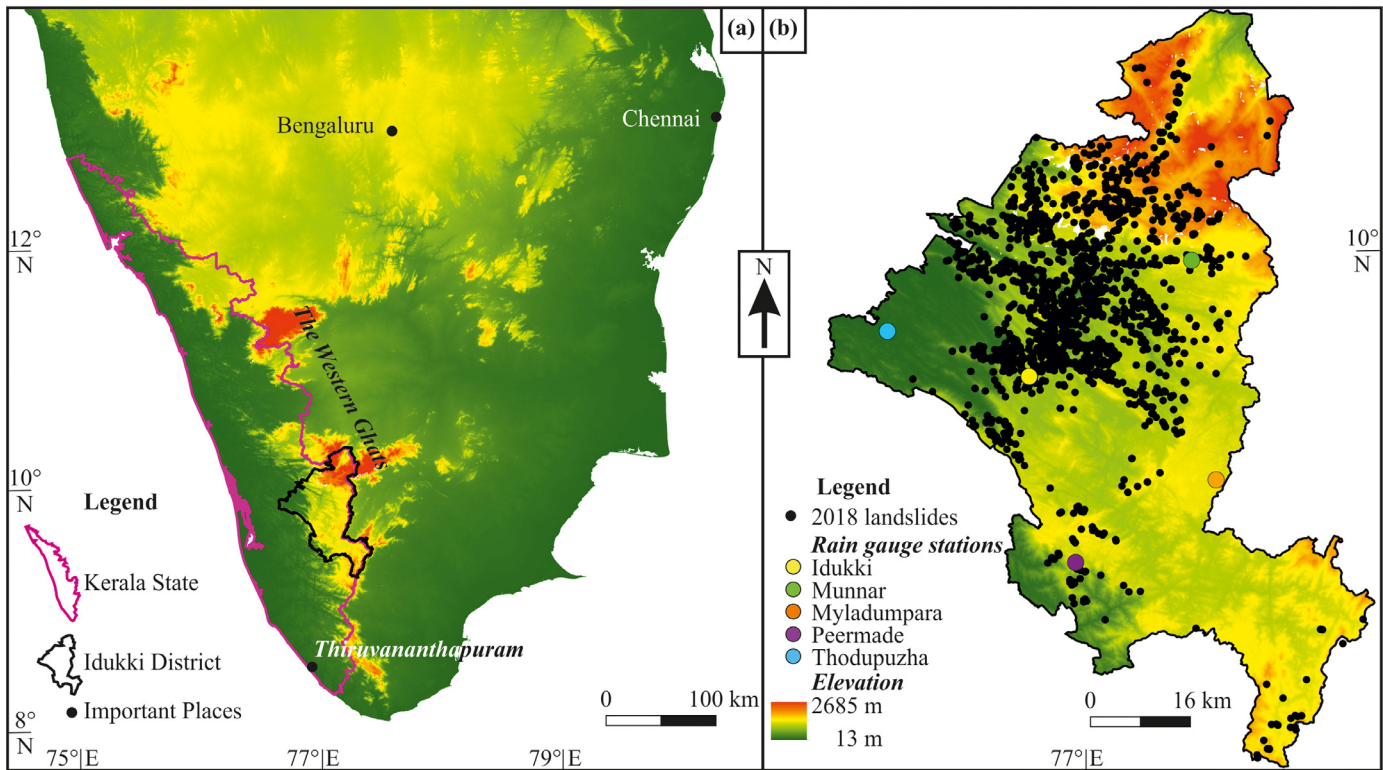


Fig. 1. Location map of the (a) Southern India (SRTM DEM in background) and (b) study area with landslide distribution (SRTM DEM draped in background).

GPM IMERG-L products for both the time steps. The short-time window of the study period was selected for this work due to the following reasons: (a) anomalous rainfall was observed during this period, and that difference is statistically significant; (b) the number of landslides is also significantly different from other duration of this year as well as any other years, and (c) sparse rain gauge networks fail to capture the spatial variability of rainfall within a short timescale.

In the next step, the satellite data was conditionally merged with the rain gauge data to improve accuracy. In this study, the conditional merging process was applied to GPM IMERG-L satellite precipitation values through four steps:

- (a) The rain gauge values were interpolated to create a continuous rain gauge-based rainfall field to obtain the best linear unbiased estimate of rainfall for all grid points (I_{rg}).
- (b) The GPM IMERG-L pixel values corresponding to the rain gauge locations were interpolated to create a continuous rainfall field (S_{rg}).
- (c) The continuous rainfall field thus obtained (S_{rg}) was differenced with the GPM IMERG-L product (S). This difference ($S - S_{rg}$) gives an error field due to interpolation, with the values at rain gauge locations being zero.
- (d) The error field obtained in step (c) is added to the rainfall field obtained in step (a). The result is a rainfall field that follows the mean field of the rain-gauge interpolation while preserving the rainfall pattern of the gridded -GPM IMERG-L information.

The final model is represented as:

$$CM = I_{rg} + S - S_{rg} \tag{1}$$

where, CM is the conditionally merged rainfall product. I_{rg} is the rain gauge interpolated rainfall field. S is the GPM IMERG-L daily rainfall product and S_{rg} is the rainfall field created from

GPM IMERG-L pixel values' interpolation corresponding to the rain gauge locations.

Fig. 2 represents the schematic diagram of the conditional merging process adopted in this study. Since the error field value is always zero at rain gauge locations, the algorithm shows the perfect conditioning to the rain values at the observed rain gauge locations. This is a unique advantage of the conditional merging algorithm over other bias-adjusted algorithms. Conditional merging is computationally efficient and robust. Since it only uses unbiased spatial interpolation, it is not affected by numerical uncertainties.

Spatial interpolation in conditional merging is generally done using kriging (Pegram and Clothier, 2001; Berndt et al., 2014; Guenzi et al., 2017; Jung et al., 2017). However, a sample data of just five rain gauges is not capable of generating any variogram shape and could lead to overestimation of spatial correlations. Thus, in this study, we resorted to using Inverse Distance Weighted (IDW) interpolation in place of kriging to create the continuous rainfall fields I_{rg} and S_{rg} . IDW interpolation was performed at the same spatial grid size as the IMERG-L data. Yang et al. (2015) compared different spatial interpolation techniques for rainfall in the Greater Sydney Region and found that IDW performs better than ANUDEM, Ordinary Kriging, and Spline. Dirks et al. (1998), Hsieh et al. (2006), Ly et al. (2010) performed comparisons of different spatial interpolation techniques for rainfall interpolation and found that IDW was better or as good as other techniques. Thus, even though IDW cannot capture anisotropy or provides error variance, due to the sparse rain gauge network and kriging's inability to generate any variogram shape with such a small number of data points, we used IDW to create interpolated surfaces required for conditional merging. The conditionally merged GPM IMERG-L data was again compared with the rain gauge data, on a daily and 5-day antecedent time step using Pearson's CC and RMSE. A cross validation of the resultant conditionally merged product was also conducted using Leave One Out

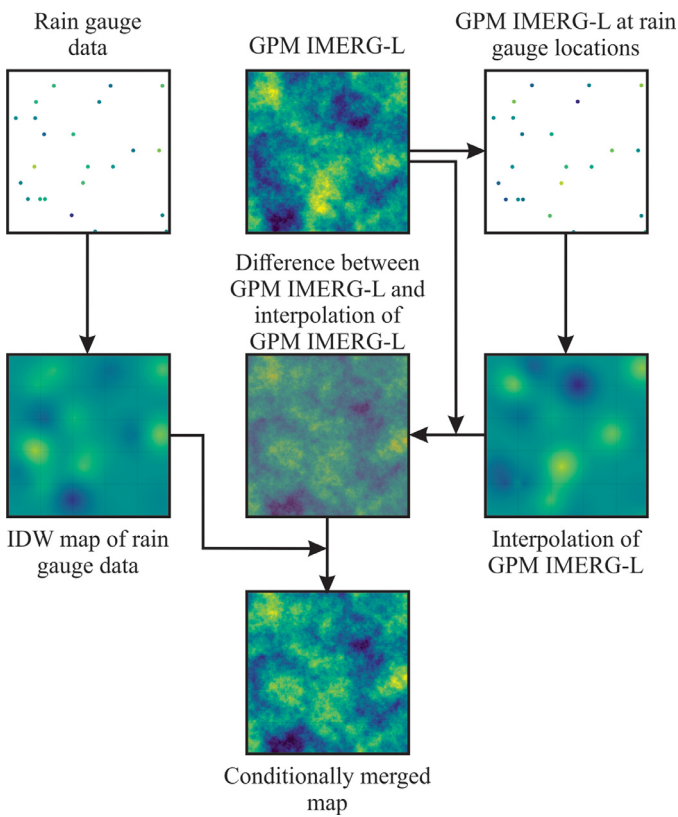
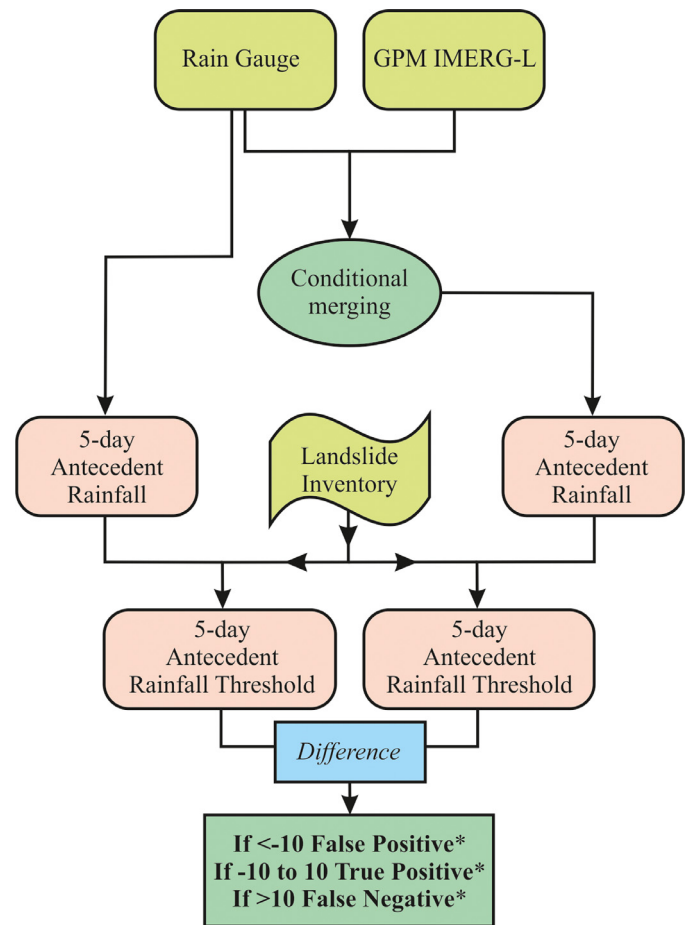


Fig. 2. Flowchart of conditional merging.

Cross-Validation (LOOCV) (Wong, 2015). In LOOCV, with k number of rain gauges, the conditional merging operations were performed k number of times, and each time, one rain gauge data was kept aside, and the remaining k-1 number of rain gauges was used to predict the CM estimated value, which was then compared with the actual rain gauge value at that location. The error, the difference between the actual value and CM estimated value, was calculated for k number of times. The error statistics from k number of error values were used to evaluate the model performance. The LOOCV ensures the validation data is never used for the CM algorithm for unbiased error calculation.

The ability of both the rain gauge derived and conditionally merged satellite rainfall products to capture landslides' spatial variability is a significant factor in developing reliable landslide prediction models. Here, the rain gauge network is sparse. Therefore, we considered a scenario where the landslide thresholds were solely derived from the rain gauge values. The satellite precipitation was used as a reference product to see how the lack of spatial variability of rain gauge-based precipitation affects the threshold computations. Idukki observed the highest rainfall on 16th August, and the peak flood was on 18th August. Since dates of landslides were not available in the landslide database, we took 17th August as a common date of occurrence of all the landslides as it falls between the day of maximum rainfall and peak flood. Thus, 5-day antecedent values corresponding to the 17th of August, derived from conditionally merged GPM IMERG-L, were compared with 5-day antecedent values derived from rain gauges. For this, the landslides were classified based on the zones of influence of each rain gauge into five distinct zones/classes. Each class had a 5-day antecedent value corresponding to that recorded by the associated rain gauge. All landslides having a conditionally merged GPM IMERG-L threshold within a range of -10 mm to +10 mm about the rain gauge threshold were considered as true positives. All other landslides having a conditionally merged GPM IMERG-L



* units in mm

Fig. 3. Flow-chart of methodology.

threshold below the rain gauge threshold were considered as false negatives and above the rain gauge threshold were considered as false positives. Fig. 3 shows a flowchart of the methodology.

4. Results

Fig. 4a shows the distribution of landslides with respect to the rain gauge stations. The blue circles in the figure show areas having high landslide frequency but occurring farther away from rain gauge stations. This is a primary indication of the inadequacy of sparse rain gauge networks to provide reliable input for any landslide prediction model in Idukki. The entire study area was divided into five Thiessen polygons, with each region falling under the influence of one rain gauge station (cf. Brassel and Reif, 1979). Fig. 4b shows the distribution of landslides over the rain gauge generated Thiessen polygons. The landslides are predominantly spread over the influence of the Idukki and Munnar rain gauge stations. The area to the north and northwest of Idukki is heavily underrepresented with rain gauges.

Satellite rainfall products have better spatial variability when compared to rain gauges. But their accuracy is debated in literature, and therefore we performed a comparison of the rain gauge and GPM IMERG-L rainfall values to check this case in Idukki. This comparison was carried out for both the daily and 5-day antecedent products. Pearson's CC and RMSE were computed for four cases: GPM IMERG-L vs rain gauge (daily), GPM IMERG-L vs rain gauge (5-day antecedent), conditionally merged GPM IMERG-L vs rain gauge (daily), and conditionally merged GPM IMERG-L vs rain gauge (5-day antecedent). The results are shown in Tables 2

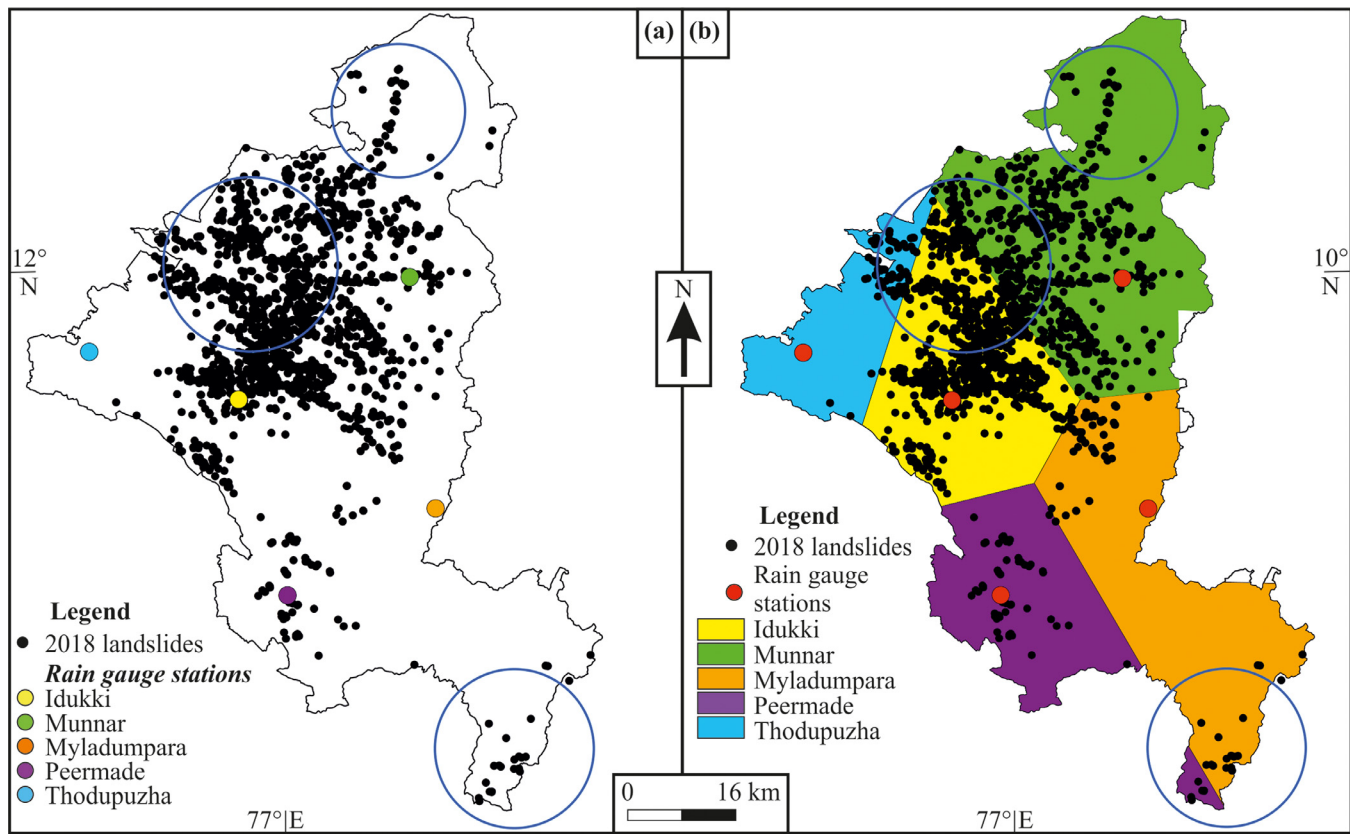


Fig. 4. Comparison of rain gauge locations and landslide distribution. (a) Landslide distribution and rain gauge locations; (b) landslide distribution and area of influence of rain gauges.

Table 2

Comparison of correlation coefficients and RMSE between GPM and rain gauge products for August 2018, for 4 scenarios: 5-day antecedent - before and after conditional merging and daily - before and after conditional merging.

	Statistic	Station1	Station2	Station3	Station4	Station5
GPM vs Rain Gauge (5-day Antecedent)	CC	0.912	0.918	0.821	0.911	0.905
	RMSE	234.52	154.47	222.80	137.02	89.27
GPM vs Rain Gauge (Daily)	CC	0.842	0.712	0.589	0.758	0.748
	RMSE	60.14	54.34	65.22	48.93	36.68
GPM CM vs Rain Gauge (5-day Antecedent)	CC	0.998	0.999	0.995	1.000	0.994
	RMSE	24.83	20.65	65.51	2.37	47.75
GPM CM vs Rain Gauge (Daily)	CC	0.984	0.997	0.974	1.000	0.983
	RMSE	16.95	4.62	20.01	0.76	12.81

Station 1-Peermade, Station 2-Thodupuzha, Station 3-Munnar, Station 4-Idukki, Station 5-Myladumpara.

CC--Coefficient of Correlation.

RMSE-Root Mean Squared Error.

and 3. From Table 2, while GPM IMERG-L has positive correlations for all stations, the daily rainfall values have a rather large range in correlation coefficients (from 0.589 to 0.842). Moreover, the 5-day antecedent rainfall values from GPM IMERG-L have a better correlation than the daily rainfall values. The comparison of RMSE values before and after conditional merging shows that the RMSE improves for both 5-day antecedent and daily rainfall values. A mean RMSE for the five stations over the 5-day antecedent values before conditional merging stands at 167.62 mm. However, upon conditional merging, this reduces to 32.22 mm while mean RMSE for daily rainfall after conditional merging reduced to 11.03 mm from a mean RMSE before conditional merging of 53.06 mm. Looking closely into the change in CC and RMSE, it is observed that the 5-day antecedent rainfall have better CC but larger RMSE prior to conditional merging. A possible explanation is that the GPM has lesser reliability on shorter temporal scales,

thereby reporting smaller CC. Since on conditional merging, the CC is improving manifold for daily rainfall, it points towards the importance of conditional merging as a process to improve the accuracy of GPM IMERG-L on a daily scale. Table 3a shows a sample case of 5-day antecedent rainfall difference between GPM IMERG-L and rain gauge measurements before and after conditional merging, on a station-wise basis. The difference in the rain gauge and GPM IMERG-L observations also fall in a large range (from 13.4 to 397.1 mm), which upon conditional merging is reduced to a range within 3.1 to 144.6 mm. The largest difference in the conditionally merged IMERG-L product was seen in the Munnar station, while the Myladumpara station observed a spike in the difference after conditional merging. However, upon observing data from the Myladumpara station for other dates, it is observed that this spike is not consistent. Table 3b analyses the rain gauge and GPM IMERG-L observations in Myladumpara (5-day

Table 3a

Comparison between rain gauge and GPM IMERG-L precipitation before and after conditional merging (for 5-day antecedent rainfall corresponding to August 17, 2018).

Station Name	Station 1	Station 2	Station 3	Station 4	Station 5
Rain gauge value (mm)	779.7	398.9	798.1	709.4	479.8
GPM Before Conditional Merging (mm)	573.5	796.0	480.4	690.5	493.2
Difference (mm)	206.2	397.1	317.7	18.9	13.4
GPM After Conditional Merging (mm)	782.6	438.5	653.5	706.3	407.2
Difference (mm)	2.9	39.6	144.6	3.1	72.6

Station 1- Peermade, Station 2- Thodupuzha, Station 3 – Munnar, Station 4 – Idukki, Station 5 – Myladumpara.

Table 3b

Comparison between rain gauge and GPM IMERG-L precipitation (5-day antecedent) before and after conditional merging for the Myladumpara station from August 13 to August 16, 2018.

Date	13 Aug	14 Aug	15 Aug	16 Aug
Rain gauge value (mm)	361.6	367	252.8	338.8
GPM Before Conditional Merging (mm)	207.6	149.1	247.1	367
Difference (mm)	148.6	217.9	5.7	28.2
GPM After Conditional Merging (mm)	274.3	313.6	186.5	282.6
Difference (mm)	87.9	53.4	66.3	56.2

Table 4

Result of leave one out cross-validation (LOOCV) for conditional merging applied over GPM IMERG-L.

Station Name	RMSE (cm)
Peermade	50.43
Thodupuzha	56.17
Munnar	57.08
Idukki	23.91
Myladumpara	21.42

antecedent) before and after conditional merging from August 13 to August 16. It is seen that while August 15 and 16 reports similar spikes as in the case of August 17, for August 13 and 14, the difference between rain gauge and GPM IMERG-L is reduced after conditional merging. However, such inconsistencies are not observed in other stations and thus, should be considered as an anomaly. This also points to the need of denser rain gauge networks so that more rain gauges with consistent data are available for gauge adjusting satellite precipitation. The complete result set with comparisons for rainfall values between the products are shown in Supplementary Data (Tables S1-S4). A line plot showing the change in GPM IMERG-L with respect to rain gauge measures before and after conditional merging is shown in Supplementary Data (Fig. S1). LOOCV was performed on the conditional merging process to ascertain its performance, and the results are shown in Table 4.

Fig. 5 shows the distribution of landslides with respect to 5-day antecedent rainfall from three data products: (a) GPM IMERG-L, (b) the conditionally merged GPM IMERG-L, and (c) IDW based interpolation of rain gauge values. In Fig. 5a, the majority of the landslides are spread across the high rainfall area, while some are spread across low rainfall areas in the south and southeast. In Fig. 5b, the landslide spread is more in accordance with the rainfall spread with most of the landslides falling in the high rainfall area. In Fig. 5c, the landslide spread is almost entirely in accordance with the rainfall spread, with little landslides falling in low rainfall pixels. However, it should be noted that pixels of similar high or low values are seen about the rain gauges as this is an interpolation product that is generated based on distance from known points as the main criteria. Thus, the IDW product will be biased towards the actual rain gauge location and may not always repre-

sent the actual spatial variability of the rainfall, unless more rain gauges are added in the network.

To further analyze the ability of the present rain gauge network to capture the spatial spread of landslides, we divided the landslides into five categories based on the area of influence of the rain gauges. Each landslide falling within a particular Thiessen polygon has a single 5-day antecedent value. On the other hand, using the conditionally merged GPM IMERG-L observed 5-day antecedent values, the landslides have a range of values. Table 5 shows the result of this comparison. A larger range indicates an increased likelihood that a landslide model would produce false positives or negatives. For example, in the area of influence of the Idukki rain gauge, 1156 landslides are recorded, having a 5-day antecedent value of 709.4 mm as recorded by the rain gauges. For a model relying solely on rain gauges, 709.4 mm will be the precipitation measure to identify the rainfall threshold in the entire area of influence of the Idukki rain gauge. However, the conditionally merged GPM IMERG-L predicts that the landslide threshold within the area of influence of the Idukki rain gauge could be as low as 532.4 mm in some places and as high as 847.9 in some places. Thus, the conditionally merged GPM IMERG-L product will identify an area having rainfall of 532.4 mm as a possible landslide occurrence, whereas the rain gauge product will identify this as a no landslide location. Similarly, the rain gauge product will identify an area with rainfall above 709.4 mm as a landslide, but if that area has a rainfall threshold of 847.9 mm for the conditionally merged GPM IMERG-L product, then it will identify that as a no landslide location. Thus, a landslide model depending solely on rain gauges would generate false negatives in areas where rainfalls are in between 532.4 and 709.4 mm and false positives in areas having rainfalls between 709.4 and 847.9 mm. In this study, false negatives can be considered as those landslides that are identified as 'no landslide location' by the rain gauge product but which are identified as landslides by conditionally merged GPM IMERG-L, while false positives are locations identified as landslides by the rain gauge product but as 'no landslide' by the conditionally merged GPM IMERG-L. However, it is to be noted that this is an exercise to point out the inadequacy of the current rain gauge locations to accurately identify spatial variations in rainfall, and we are not making a statement that GPM IMERG-L conditionally merged or otherwise represents the exact values of actual rainfall.

To further support this finding, we have computed the number of false positives, false negatives, and true positives falling within

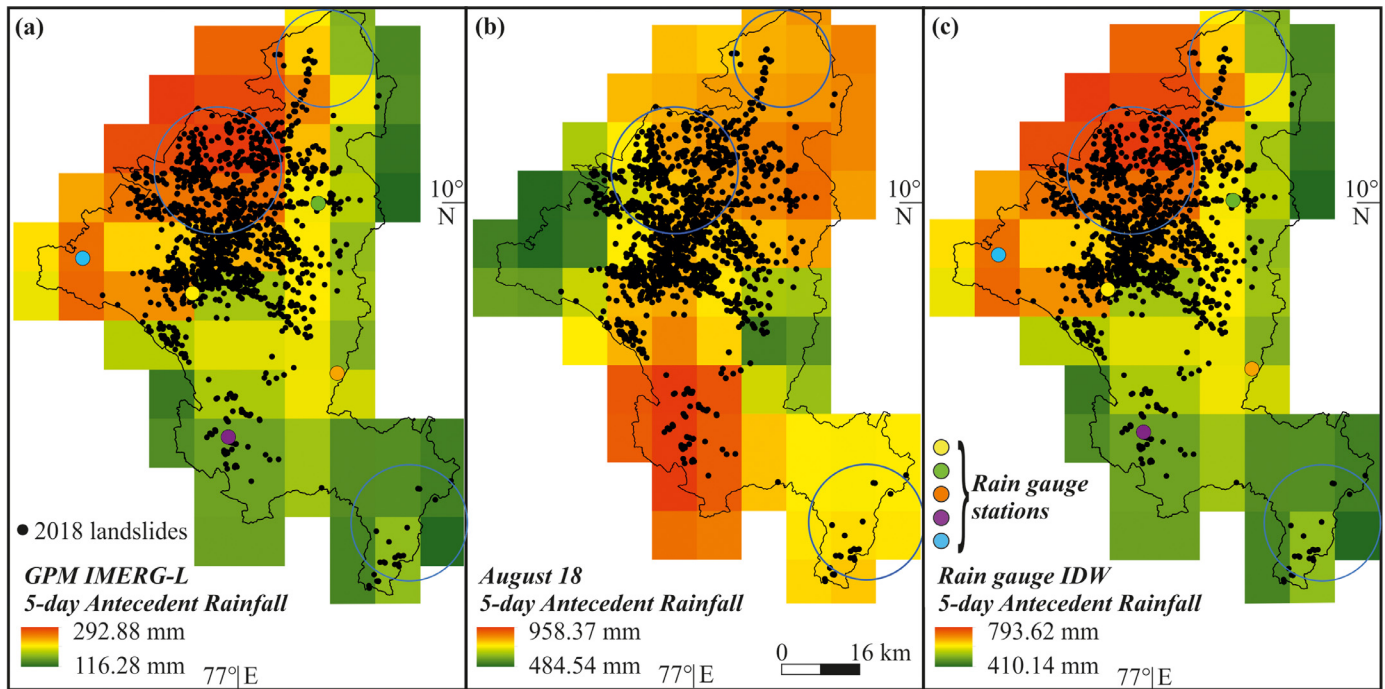


Fig. 5. (a) GPM IMERG-L 5-day antecedent rainfall product and landslide distribution. (b) Comparison of conditionally merged GPM IMERG-L 5-day antecedent rainfall product and landslide distribution. (c) Comparison of IDW interpolated rain gauge product for 5-day antecedent rainfall and landslide distribution. The blue circles show the region where there is landslide activity but have clear underrepresentation of rain gauges. The 5-day antecedent rainfall corresponds to August 17, 2018.

Table 5
Comparison of 5-day antecedent rainfall values between rain gauge and conditionally merged GPM IMERG-L.

Station Name	No. of Landslides	5-day antecedent value (mm)	5-day antecedent range for landslides from GPM (mm)	Range (mm)
Idukki	1156	709.4	532.4 – 847.9	315.5
Munnar	843	798.1	463.3 – 847.9	384.6
Myladumpara	71	479.8	434.8 – 602.5	167.7
Peermade	75	779.7	476.6 – 782.6	306.0
Thodupuzha	78	398.9	438.4 – 847.9	409.5

Table 6
Landslide classification statistics based on the scenario were the rain gauge measures are solely relied upon.

Station Name	Number of landslides		
	False Positives	True Positives	False Negatives
Idukki	237	376	543
Munnar	92	0	751
Myladumpara	53	5	13
Peermade	1	34	40
Thodupuzha	78	0	0
Total	461	415	1347

the area of influence of each rain gauge. True positives are considered for all landslides with a rainfall value within a range of -10 mm to +10 mm from the rain gauge observed rainfall threshold. All other values falling below the rain gauge observed threshold are counted as false negatives and all other values falling above the rain gauge observed threshold are counted as false positives. Table 6 classifies the landslides into false negatives, true positives, and false positives, falling under each rain gauge station’s area of influence. A total of 1347 landslides fall in the false-negative category, while there are 461 false positives and 415 true positives. Such a scenario will give rise to 18.7% true-positives, while the false-negative rate is 60.7%. Munnar records the highest false-negative rate out of the five stations with 89.1% while having zero

true positives. Thodupuzha records a 100% false-positive rate. Fig. 6 is a graphical representation of this scenario.

5. Discussion

A comparison of the landslide database and the rain gauge locations showed that the existing rain gauge network has limited capability to cover the landslide spread. More rain gauges are required to accurately capture the spatial variations in rainfall as well as provide more reliable input for landslide monitoring. The ability of satellite rainfall products to be used as an alternative was checked using the rainfall measurements from GPM IMERG-L. However, it was found that GPM IMERG-L was underpredicting the rainfall and thus, a conditional merging process was applied to improve its accuracy.

The GPM IMERG-L and rain gauge products were compared before and after conditional merging, and correlation coefficients and RMSE were calculated. A general reduction in RMSE and improvement in correlation with rain gauge values were seen after performing the conditional merging, and this point towards the efficacy of the method in improving the accuracy of GPM IMERG-L precipitation measure in the study area.

The conditional merging process was subjected to a LOOCV as a means of validating the process. The result of the LOOCV indicates that Myladumpara has the least RMSE while Munnar records the maximum. The RMSE values range from 21.42 to 57.08. The large

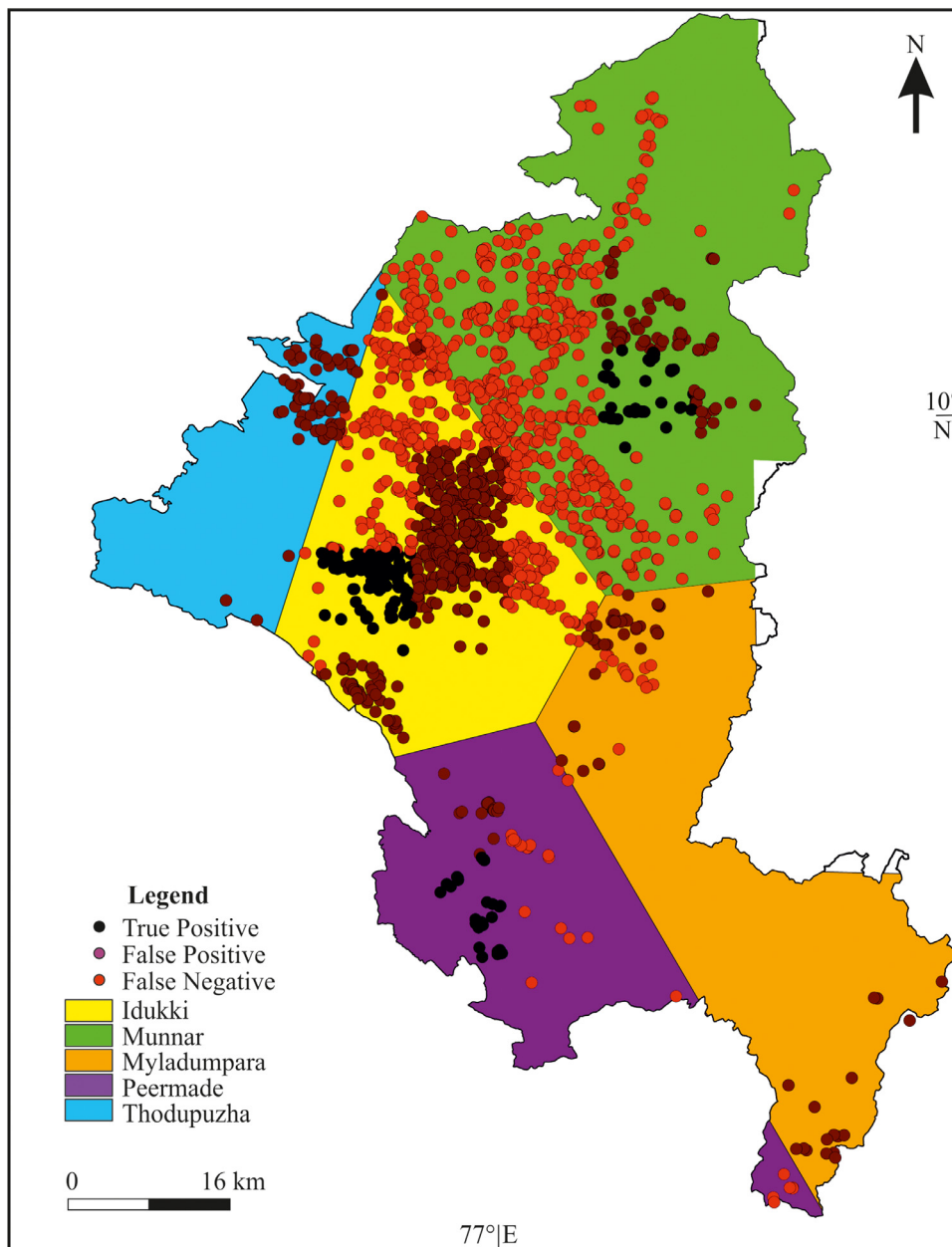


Fig. 6. Representation of landslide classification statistics for a scenario in which only rain gauge measurements are relied upon for modeling.

difference in RMSE is indicative of the large spatial variation in rainfall and the inadequate spread of rain gauge stations to capture it, as leaving out certain stations contributes to a larger error than other stations.

Comparing the spatial spread of landslides with three rainfall products viz., (a) GPM IMERG-L, (b) conditionally merged GPM IMERG-L, and (c) IDW interpolated rain gauge product, showed that the conditionally merged product captures the spatial spread of landslides better than the unconditioned one. Although the IDW interpolated rain gauge product conformed to the landslide pattern better than the other products, it showed a bias towards the rain gauge locations evidently showing the lack of spatial variations.

An example scenario that took 5-day antecedent rainfall for the 17th of August as a rainfall threshold to trigger landslides was considered and compared with the rain gauge and conditionally merged GPM IMERG-L products. This showed that relying solely on rain gauges for landslide monitoring would result in threshold

values that may fall far off from the actual scenario and result in many false positives and false negatives. However, GPM IMERG-L could not be relied upon alone as well as it underpredicts rainfall, and rain gauge observations are required to condition them. This points to the need to improve the existing rain gauge network by installing new rain gauges in locations that can optimally capture landslide activity. GPM IMERG-L can be used as a continuous dataset as any number of rain gauges would still result in a discrete dataset, and interpolating them would still give products that are biased towards the rain gauge locations.

Another point of concern in adopting GPM IMERG-L is its spatial resolution. The GPM IMERG-L has a coarse spatial resolution of about 10 km, which will be inadequate to capture the scale of landslides. For example, the 5-day antecedent rainfall values obtained from the conditionally merged GPM IMERG-L had 38 unique values, each corresponding to one pixel. This would indicate an average of 58.5 landslides per pixel. Such a spatial resolution is still

not representative of capturing the spread of landslides in Idukki, and thus data of better spatial resolution is required to have further accurate models.

6. Conclusions

The study probed the utility of rain gauge and satellite rainfall data for developing a landslide prediction model in Idukki. The study area had sparse rain gauge density with only five rain gauges for 4366 sq. km. GPM IMERG-L daily rainfall product was underpredicting rainfall when compared with ground-based rain gauge data. However, on applying a conditional merging process, the rain gauge and satellite rainfall products were merged to create a rainfall product that preserved the accuracy of the rain gauge and the spatial variability of GPM IMERG-L. A comparison between GPM IMERG-L, conditionally merged GPM IMERG-L and IDW interpolated rain gauge products showed that the interpolated product captured the spatial spread of landslides best, followed by the conditionally merged GPM IMERG-L. However, the interpolated product is biased towards the rain gauge locations and is thus, not reliable in a sparse rain gauge network. An example scenario that considered a rain gauge-based threshold for landslide trigger found that such a model would result in many false negatives and false positives and will not provide reliable precipitation information for a landslide prediction model.

It can be concluded that conditional merging the GPM IMERG-L with rain gauge observations will improve its accuracy. However, sparse rain gauge networks affect the efficacy of this process as well as rainfall thresholds derived for landslide modeling. Sparse rain gauges impede the conditional merging process as locations farther away from the rain gauges may have large variations from accurate rainfall values. Moreover, the spatial resolution of GPM IMERG-L is inadequate to capture the landslide occurrences in Idukki. Thus, future work should be focused on the direction of improving the existing rain gauge network by installing new rain gauges at optimal locations and improving the spatial resolution of GPM IMERG-L. The installation of new rain gauges would facilitate the better prediction of rainfall over Idukki, thereby aiding landslide and rainfall modelling systems, ultimately providing credible early warning to the population.

Declaration of Competing Interest

The authors declare that they have no known competing financial interests or personal relationships that could have appeared to influence the work reported in this paper.

Acknowledgments

The authors acknowledge the Society of Exploration Geophysicists (SEG) Geoscientists Without Borders (GWB) funded this study (SEG GWB #201907008).

Supplementary materials

Supplementary material associated with this article can be found, in the online version, at doi:[10.1016/j.geogeo.2022.100060](https://doi.org/10.1016/j.geogeo.2022.100060).

References

- Abraham, P.B., Shaji, E., 2013. Landslide hazard zonation in and around Thodupuzha-Idukki-Munnar road, Idukki district, Kerala: a geospatial approach. *J. Geol. Soc. India* 82 (6), 649–656.
- Arnone, E., Noto, L.V., Lepore, C., Bras, R.L., 2011. Physically based and distributed approach to analyze rainfall-triggered landslides at watershed scale. *Geomorphology* 133, 121–131.
- Berndt, C., Rabiei, E., Haberlandt, U., 2014. Geostatistical merging of rain gauge and radar data for high temporal resolutions and various station density scenarios. *J. Hydrol.* 508, 88–101 (Amst).
- Boushaki, F.I., Hsu, K.L., Sorooshian, S., Park, G.H., Mahani, S., Shi, W., 2009. Bias adjustment of satellite precipitation estimation using ground-based measurement: a case study evaluation over the southwestern United States. *J. Hydrometeorol.* 10 (5), 1231–1242.
- Brassel, K.E., Reif, D., 1979. A procedure to generate Thiessen polygons. *Geogr. Anal.* 11 (3), 289–303.
- Brunetti, M.T., Melillo, M., Peruccacci, S., Ciabatta, L., Brocca, L., 2018. How far are we from the use of satellite rainfall products in landslide forecasting? *Remote Sens. Environ.* 210, 65–75.
- Brunetti, M.T., Melillo, M., Gariano, S.L., Ciabatta, L., Brocca, L., Amarnath, G., Peruccacci, S., 2021. Satellite rainfall products outperform ground observations for landslide prediction in India. *Hydrol. Earth Syst. Sci.* 25 (6), 3267–3279.
- Crozier, M.J., 1999. Prediction of rainfall-triggered landslides: a test of the antecedent water status model. *Earth Surf. Process. Landf.* 24, 825–833.
- Dash, N., Gladwin, H., 2007. Evacuation decision making and behavioral responses: individual and household. *Nat. Hazard. Rev.* 8 (3), 69–77.
- Dietrich, W.E., Montgomery, D.R., 1998. SHALSTAB: A Digital Terrain Model For Mapping Shallow Landslide Potential. University of California.
- Dirks, K.N., Hay, J.E., Stow, C.D., Harris, D., 1998. High-resolution studies of rainfall on Norfolk Island: part II: interpolation of rainfall data. *J. Hydrol.* 208 (3–4), 187–193 (Amst).
- Dirksen, C., Kool, J.B., Koorevaar, P., Van Genuchten, M.T., 1993. HYSWASOR-Simulation model of hysteretic water and solute transport in the root zone. In: *In Water Flow and Solute Transport in Soils*. Springer, Berlin, Heidelberg, pp. 99–122.
- Froude, M.J., Petley, D.N., 2018. Global fatal landslide occurrence from 2004 to 2016. *Nat. Hazards Earth Syst. Sci.* 18, 2161–2181.
- Gairola, R.M., Prakash, S., Pal, P.K., 2015. Improved rainfall estimation over the Indian monsoon region by synergistic use of Kalpana-1 and rain gauge data. *Atmosfera* 28 (1), 51–61.
- Garstang, M., Kummerow, C.D., 2000. The Joanne Simpson special issue on the Tropical Rainfall Measuring Mission (TRMM). *J. Appl. Meteorol.* 39 (12), 1961.
- Glade, T., Crozier, M., Smith, P., 2000. Applying probability determination to refine landslide-triggering rainfall thresholds using an empirical "antecedent daily rainfall model". *Pure Appl. Geophys.* 157, 1059–1079.
- Guarascio, M., Folino, G., Chiaravalloti, F., Gabriele, S., Procopio, A., Sabatino, P., 2020. A machine learning approach for rainfall estimation integrating heterogeneous data sources. *IEEE Trans. Geosci. Remote Sens.* 60, 4200111.
- Guenzi, D., Fratianni, S., Boraso, R., Cremonini, R., 2017. CondMerg: an open source implementation in R language of conditional merging for weather radars and rain gauges observations. *Earth Sci Inform* 10 (1), 127–135.
- Guzzetti, F., Malamud, B.D., Turcotte, D.L., Reichenbach, P., 2002. Power-law correlations of landslide areas in central Italy. *Earth Planet. Sci. Lett.* 195 (3–4), 169–183.
- Hao, L., van Westen, C., Rajaneesh, A., Sajinkumar, K.S., Martha, T.R., Jaiswal, P., McAdoo, B., 2020. Constructing a complete landslide inventory dataset for the 2018 Monsoon disaster in Kerala, India, for land use change analysis. *Earth Syst. Sci. Data Discuss.* 12 (4), 2899–2918.
- Hong, Y., Adler, R.F., 2008. Predicting global landslide spatiotemporal distribution: integrating landslide susceptibility zoning techniques and real-time satellite rainfall estimates. *Int. J. Sediment Res.* 23, 249–257.
- Hong, Y., Adler, R.F., Huffman, G., 2007. An experimental global prediction system for rainfall-triggered landslides using satellite remote sensing and geospatial datasets. *IEEE Trans. Geosci. Remote Sens.* 45 (6), 1671–1680.
- Hou, A.Y., Kakar, R.K., Neeck, S., Azarbarzin, A.A., Kummerow, C.D., Kojima, M., Iguchi, T., 2014. The global precipitation measurement mission. *Bull. Am. Meteorol. Soc.* 95 (5), 701–722.
- Hsieh, H.H., Cheng, S.J., Liou, J.Y., Chou, S.C., Siao, B.R., 2006. Characterization of spatially distributed summer daily rainfall. *J. Chin. Agric. Eng.* 52 (1), 47–55.
- Iverson, R.M., 2000. Landslide triggering by rain infiltration. *Water Resour. Res.* 36 (7), 1897–1910.
- Jennifer, J.J., Saravanan, S., 2021. Artificial neural network and sensitivity analysis in the landslide susceptibility mapping of Idukki district, India. *Geocarto Int.* doi:[10.1080/10106049.2021.1923831](https://doi.org/10.1080/10106049.2021.1923831).
- Joshi, M.K., Rai, A., Pandey, A.C., 2013. Validation of TMPA and GPCP 1DD against the ground truth rain-gauge data for Indian region. *Int. J. Climatol.* 33 (12), 2633–2648.
- Jones, S., Kasthurba, A.K., Bhagyanathan, A., Binoy, B.V., 2021. Landslide susceptibility investigation for Idukki district of Kerala using regression analysis and machine learning. *Arabian J. Geosci.* 14 (10), 1–17.
- Jung, C., Lee, Y., Cho, Y., Kim, S., 2017. A study of spatial soil moisture estimation using a multiple linear regression model and MODIS land surface temperature data corrected by conditional merging. *Remote Sens.* 9 (8), 870 (Basel).
- Kim, D., Im, S., Lee, S.H., Hong, Y., Cha, K.S., 2010. Predicting the rainfall-triggered landslides in a forested mountain region using TRIGRS model. *J. Mt. Sci.* 7 (1), 83–91.
- Kirschbaum, D., Stanley, T., 2018. Satellite-based assessment of rainfall-triggered landslide hazard for situational awareness. *Earth's Future* 6, 505–523.
- Kuriakose, S.L., Sankar, G., Muraleedharan, C., 2009. History of landslide susceptibility and a chorology of landslide-prone areas in the Western Ghats of Kerala, India. *Environ. Geol.* 57 (7), 1553–1568.
- Lamb, R., Beven, K., Myrabo, S., 1998. Use of spatially distributed water table observations to constrain uncertainty in a rainfall-runoff model. *Adv. Water Resour.* 22 (4), 305–317.
- Larsen, M.C., Simon, A., 1993. A rainfall intensity duration threshold for landslides in a humid tropical environment, Puerto Rico. *Geogr. Ann. Phys. Geogr.* 75 (1/2), 13–23.

- Lepore, C., Arnone, E., Noto, L.V., Sivandran, G., Bras, R.L., 2013. Physically based modeling of rainfall-triggered landslides: a case study in the Luquillo forest, Puerto Rico. *Hydrol. Earth Syst. Sci.* 17 (9), 3371–3387.
- Liu, Z., Ostrenga, D., Teng, W., Kempler, S., 2012. Tropical Rainfall Measuring Mission (TRMM) precipitation data and services for research and applications. *Bull. Am. Meteorol. Soc.* 93 (9), 1317–1325.
- Liu, Z., Ostrenga, D., Vollmer, B., Deshong, B., Macritchie, K., Greene, M., Kempler, S., 2017. Global precipitation measurement mission products and services at the NASA GES DISC. *Bull. Am. Meteorol. Soc.* 98 (3), 437–444.
- Ly, S., Charles, C., Degré, A., 2010. Spatial interpolation of daily rainfall at catchment scale: a case study of the Ourthe and Ambleve catchments, Belgium. *HESSD* 7 (5), 7383–7416.
- Mackie, B. (2014). Warning fatigue: insights from the Australian bushfire context. (Unpublished thesis), University of Canterbury.
- Marra, F., Nikolopoulos, E.I., Creutin, J.D., Borga, M., 2014. Radar rainfall estimation for the identification of debris-flow occurrence thresholds. *J. Hydrol.* 519, 1607–1619 (Amst).
- Mishra, A.K., 2013. Effect of rain gauge density over the accuracy of rainfall: a case study over Bangalore, India. *SpringerPlus* 2 (1), 1–7.
- Naidu, S., Sajinkumar, K.S., Oommen, T., Anuja, V.J., Samuel, Rinu A., Muraliedharan, C., 2018. Early warning system for shallow landslides using rainfall threshold and slope stability analysis. *Geosci. Front.* 9 (6), 1871–1882.
- Nikolopoulos, E.I., Destro, E., Maggioni, V., Marra, F., Borga, M., 2017. Satellite rainfall estimates for debris flow prediction: an evaluation based on rainfall accumulation-duration thresholds. *J. Hydrometeorol.* 18 (8), 2207–2214.
- Pack, R.T., Tarboton, D.G., Goodwin, C.N., 2007. Assessing terrain stability in a GIS using SINMAP.
- Parida, B.R., Behera, S.N., Bakimchandra, O., Pandey, A.C., Singh, N., 2017. Evaluation of satellite-derived rainfall estimates for an extreme rainfall event over Uttarakhand, Western Himalayas. *Hydrology* 4 (2), 22.
- Pegram, G.G.S., Clothier, A.N., 2001. High resolution space-time modelling of rainfall: the "String of Beads" model. *J. Hydrol.* 241 (1–2), 26–41 (Amst).
- Pradhan, A., Indu, J., 2021. Assessment of SM2RAIN derived and IMERG based precipitation products for hydrological simulation. *J. Hydrol.* 603, 127191 (Amst).
- Prakash, S., Mitra, A.K., Momin, I.M., Rajagopal, E.N., Basu, S., Collins, M., ..., Ashok, K., 2015. Seasonal intercomparison of observational rainfall datasets over India during the southwest monsoon season. *Int. J. Climatol.* 35 (9), 2326–2338.
- Prakash, S., Seshadri, A., Srinivasan, J., Pai, D.S., 2019. A new parameter to assess impact of rain gauge density on uncertainty in the estimate of monthly rainfall over India. *J. Hydrometeorol.* 20 (5), 821–832.
- Rajeevan, M., Bhate, J., 2009. A high resolution daily gridded rainfall dataset (1971–2005) for mesoscale meteorological studies. *Curr. Sci.* 6 (4), 558–562.
- Robbins, J.C., 2016. A probabilistic approach for assessing landslide-triggering event rainfall in Papua New Guinea, using TRMM satellite precipitation estimates. *J. Hydrol.* 541, 296–309 (Amst).
- Rossi, M., Kirschbaum, D., Luciani, S., Mondini, A.C., Guzzetti, F., 2012. TRMM satellite rainfall estimates for landslide early warning in Italy: preliminary results. In: *Remote Sensing of the Atmosphere, Clouds, and Precipitation IV*, 8523. International Society for Optics and Photonics, p. 85230. doi:10.1117/12.979672.
- Sajinkumar, K.S., Anbazhagan, S., Pradeepkumar, A.P., Rani, V.R., 2011. Weathering and landslide occurrences in parts of Western Ghats, Kerala. *J. Geol. Soc. India* 78 (3), 249.
- Sajinkumar, K.S., Arya, A., Rajaneesh, A., Oommen, T., Yunus, Ali.P., Rani, V.R., Avatar, Ram, Thirivikramji, K.P., 2022. Migrating rivers, consequent paleochannels: the unlikely partners and hotspots of flooding. *Sci. Total Environ.* 807, 150842.
- Sajinkumar, K.S., Oommen, T., 2020. Rajamala landslide: continuation of a never-ending landslide series. *J. Geol. Soc. India* 96, 310.
- Sajinkumar, K.S., Oommen, T., 2021. In: *Landslide Atlas of Kerala*, 7. Geological Society of India, Bangalore, p. 34.
- Sajinkumar, K.S., Rinu, S., Oommen, T., Vishnu, C.L., Praveen, K.R., Rani, V.R., Muraliedharan, C., 2020. Improved rainfall threshold for landslides in data sparse and diverse geomorphic milieu: a cluster analysis based approach. *Nat. Hazards J. Int. Soc. Prev. Mitig. Nat. Hazards* 103, 639–657.
- Sidle, R., Ochiai, H., 2006. Processes, Prediction, and Land Use. *Water resources Monograph*. American Geophysical Union, Washington.
- Sinclair, S., Pegram, G., 2005. Combining radar and rain gauge rainfall estimates using conditional merging. *Atmos. Sci. Lett.* 6 (1), 19–22.
- Sorensen, J.H., Sorensen, B.V., 2007. Community Processes: Warning and Evacuation. In *Handbook of Disaster Research*. Springer, New York, NY (pp. 183–199).
- Stanley, T., Kirschbaum, D.B., 2017. A heuristic approach to global landslide susceptibility mapping. *Nat. Hazards* 87 (1), 145–164.
- Sun, W., Sun, Y., Li, X., Wang, T., Wang, Y., Qiu, Q., Deng, Z., 2018. Evaluation and correction of GPM IMERG precipitation products over the capital circle in North-east China at multiple spatiotemporal scales. *Adv. Meteorol.* doi:10.1155/2018/4714173.
- Sungmin, O., Kirstetter, P.E., 2018. Evaluation of diurnal variation of GPM IMERG-derived summer precipitation over the contiguous US using MRMS data. *Q. J. R. Meteorol. Soc.* 144, 270–281.
- Tang, G., Clark, M.P., Papalexiou, S.M., Ma, Z., Hong, Y., 2020. Have satellite precipitation products improved over last two decades? A comprehensive comparison of GPM IMERG with nine satellite and reanalysis datasets. *Remote Sens. Environ.* 240, 111697.
- Terlien, M.T.J., 1998. The determination of statistical and deterministic hydrological landslide-triggering thresholds. *Environ. Geol.* 35 (2–3), 124–130.
- Thampi, P.K. (1997). Evaluation study in terms of landslide mitigation in parts of Western Ghats Kerala, India. *Centre for Earth Science Studies*.
- Tobin, K.J., Bennett, M.E., 2010. Adjusting satellite precipitation data to facilitate hydrologic modeling. *J. Hydrometeorol.* 11 (4), 966–978.
- Vignal, B., Krajewski, W.F., 2001. Large-sample evaluation of two methods to correct range-dependent error for WSR-88D rainfall estimates. *J. Hydrometeorol.* 2 (5), 490–504.
- Vishnu, C.L., Sajinkumar, K.S., Oommen, T., Coffman, R.A., Thirivikramji, K.P., Rani, V.R., Keerthy, S., 2019. Satellite-based assessment of the August 2018 flood in parts of Kerala, India. *Geomat. Nat. Hazards Risk* 10 (1), 758–767.
- Vishnu, C.L., Rani, V.R., Sajinkumar, K.S., Oommen, T., Bonali, F.L., Pareeth, S., Rajaneesh, A., 2020. Catastrophic flood of August 2018, Kerala, India: study of partitioning role of lineaments in modulating flood level using remote sensing data. *Remote Sens. Appl. Soc. Environ.* 20, 100426.
- Wadhawan, S.K., Singh, B., Ramesh, M.V., 2020. Causative factors of landslides 2019: case study in Malappuram and Wayanad districts of Kerala, India. *Landslides* 17, 2689–2697.
- Woldemeskel, F.M., Sivakumar, B., Sharma, A., 2013. Merging gauge and satellite rainfall with specification of associated uncertainty across Australia. *J. Hydrol.* 499, 167–176 (Amst).
- Wong, T.T., 2015. Performance evaluation of classification algorithms by k-fold and leave-one-out cross validation. *Pattern Recognit.* 48 (9), 2839–2846.
- Yang, X., Xie, X., Liu, D.L., Ji, F., Wang, L., 2015. Spatial interpolation of daily rainfall data for local climate impact assessment over greater Sydney region. *Adv. Meteorol.* doi:10.1155/2015/563629, 2015.
- Zambrano-Bigiarini, M., Nauditt, A., Birkel, C., Verbist, K., Ribbe, L., 2017. Temporal and spatial evaluation of satellite-based rainfall estimates across the complex topographical and climatic gradients of Chile. *Hydrol. Earth Syst. Sci.* 21 (2), 1295–1320.
- Zhao, H., Yang, B., Yang, S., Huang, Y., Dong, G., Bai, J., Wang, Z., 2018. Systematical estimation of GPM-based global satellite mapping of precipitation products over China. *Atmos. Res.* 201, 206–217.